

Friedrich Schiller Universität Jena
PAF

Dissertation

High-Fluence Ion Beam Irradiation of Semiconductor Nanowires

Andreas Johannes

März 2015

Abstract

Hier alles Bla

Contents

1	Introduction	1
2	High Doping Concentrations in Nanowires	2
2.1	Doping and Sputtering	2
2.2	nano-XRF on single nanowires	5
2.3	Pseudo-dynamic simulation	8
2.4	Discussion of relevant effects	8
3	Summary and Outlook	10

1 Introduction

2 High Doping Concentrations in Nanowires

This chapter will discuss the concentration of dopants incorporated into ion irradiated nanowires. The simulations and experiments presented in this chapter were all performed on Mn^+ irradiated ZnO nanowires, however the effects are easily applied to other material combinations. Some of the first results were published in reference [JNP⁺14].

2.1 Doping and Sputtering

With *iradiana* the distribution of the places where the ions come to rest gives the profile of the concentration of dopants per fluence. Locally the concentration [$atoms/cm^3$] increases a certain amount per fluence [$ions/cm^2$], leading to the somewhat awkward unit of for the doping efficacy [$(atoms/cm^3)/(ions/cm^2)$]. An example of the dopant distribution simulated with *iradina* is shown in figure 2.1a for the irradiation of a ZnO nanowire with $175\ keV\ Mn^+$. The ions enter the y - z plane at random locations and at an angle of 45° to the z -axis, which is periodically continued outside the plane of the image. It is clear that a homogeneous doping profile is not easy to obtain for the irradiation of a nanowire from one side. As with the creation of a box profile in bulk irradiation, multiple irradiation steps with varying energy are required. Note that an ion energy of

2.1 Doping and Sputtering

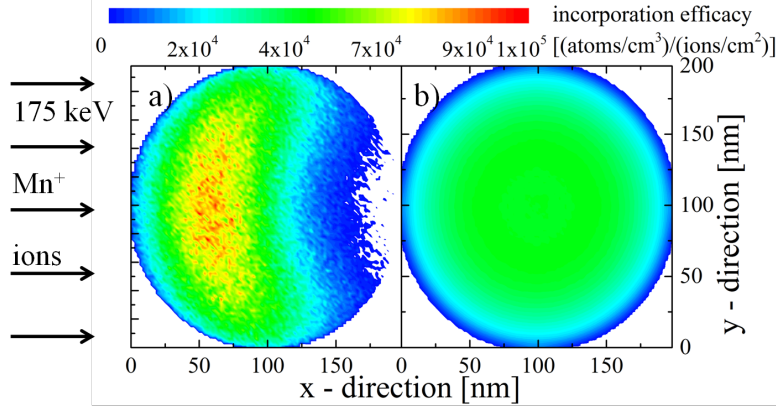


Figure 2.1: a) Color plot of the increase in concentration per fluence for the irradiation of a ZnO nanowire with $175\text{ keV } Mn^+$ ions at an angle of 45° to the z -axis. The energy was selected so that the rotation of this profile produces a radially homogeneous dopant distribution, as shown in b). The mean dopant incorporation efficacy is $3.6 \cdot 10^4 \text{ (atoms/cm}^3\text{)/(ion/cm}^2\text{)}$.

175 keV is obviously not enough to permeate the whole nanowire diameter of 200 nm , so that an additional irradiation with higher ion energy would be required to obtain homogeneous doping. Rotating the nanowire under the ion beam is a much easier way of increasing homogeneity of the doping profile. Figure 2.1b shows the local dopant incorporation efficacy for the rotation of the profile shown in 2.1a. Irradiation with a single, relatively low ion energy produces a homogeneous doping profile.

As lower energy ions have lower ranges, there are fewer paths that cause the ion to leave the nanowire, particularly in the forward direction. Therefore, the first advantage of decreasing the ion energy is that the doping efficacy is larger for lower ion energies, so a lower irradiation fluence is required to achieve doping at a desired level. Furthermore, lower ion energy impacts also produce less damage in the irradiated matrix. Together with an optimal irradiation temperature, the rotated irradiation

2 *High Doping Concentrations in Nanowires*

tion was utilized to improve the magnetic properties of Mn^+ irradiated *GaAs* nanowires [BMB⁺11, PKB⁺12, Bor12, KPJ⁺13, PKJ⁺14].

The assumption underlying the doping efficacy and using it to calculate the required fluence for a desired doping concentration is that the concentration increases linearly with the irradiated fluence. This is only true in the absence of sputtering. In figure 2.1b the outermost layer of the nanowire has a lower dopant incorporation efficacy than the rest of the wire volume. The sputtered atoms predominantly originate from this outer layer, so that the matrix of the nanowire is eroded preferentially to the incorporated dopants. Sputtering therefore leads to a non-linear increase in the concentration of dopants with the irradiated fluence.

2.2 nano-XRF on single nanowires

The expected non-linear increase in doping concentration with the ion fluence was first investigated on *ZnO* nanowire samples grown in Jena, such as the one shown in figure ??a. The nanowires were transferred onto the carbon-foil of a *Cu* TEM grid by imprinting after the rotated irradiation with 0.24, 0.48, 0.95 and $1.9 \cdot 10^{17} \text{ ions/cm}^2$ Mn^+ ions at 175 keV; corresponding to *Mn/Zn* ratios of 0.02, 0.04, 0.08 and 0.16, as extrapolated from the mean doping efficacy obtained from the *iradina* simulation.

Figure 2.2a shows a SEM image of one of the Mn^+ irradiated *ZnO* nanowires investigated by nano-XRF at the ESRF. At one point the nanowire shows some damage where the exposure to the XRF-beam was prolonged during the navigation on the sample. Also the track of the intense, focused X-ray beam can be seen on the carbon foil by some redeposition of material. All in all, the damage to the nanowire is, however, not large enough to have an effect on the quantification, especially considering that this particular nanowire was selected as it showed the most pronounced effects. In 2.2b a map of the detected X-ray intensity clearly shows the nanowire. The XRF spectrum collected for one of the scans indicated in the SEM image 2.2a is shown in 2.2c. The number of counts for a single scan is comfortably sufficient to quantify the *Mn* and *Zn* content. The average concentration for a nanowire was determined by fitting the sum XRF-spectrum of all scans across the nanowire. The *Mn/Zn* ratio is plotted over the position along the nanowire for the four nominal concentrations in figure 2.2d. Clearly there is a significant gradient in the *Mn* concentration along the nanowire length. The maximum *Mn/Zn* ratio was always found at the tip of the nanowire, which was identifiable in the SEM images by the slight tapering of the nanowires. The *Mn/Zn* ratio for both the sum of all scans, as well as the scan at the tip showing the maximum *Mn/Zn* ratio

2 *High Doping Concentrations in Nanowires*

is plotted in 2.2e alongside the nominal ratio extrapolated from *iradina* simulations.

2.3 Pseudo-dynamic simulation

The direct simulation of the effect of sputtering on the incorporation of dopants into nanowires requires a dynamic simulation program, which also considers the three dimensional geometry of the target. However, with results from many static simulations for varying diameters, a pseudo-dynamic study can be conceived. The sputter yield is dependent on the nanowire radius and the ion energy as shown in 2.3a. This relation is discussed in detail in the previous chapter ???. Likewise the incorporation efficacy plotted in 2.3b is also dependent on the nanowire radius and the ion energy. For a fixed diameter and increasing ion energy the efficacy is monotonically decreasing, as the probability of the ion to leave the nanostructure rises together with the ion range. For fixed ion energies the probability of an ion to stay in the nanostructure increases with increasing diameter, so that at first the efficacy also increases with increasing diameter. For large diameters this effect is overcompensated by a stronger dilution of the dopants in the volume of the nanowire which increases as the square of the diameter. This leads to a maximum in the incorporation efficacy at diameters around twice the ion range.

2.4 Discussion of relevant effects

Summarizing Discussion

2 High Doping Concentrations in Nanowires

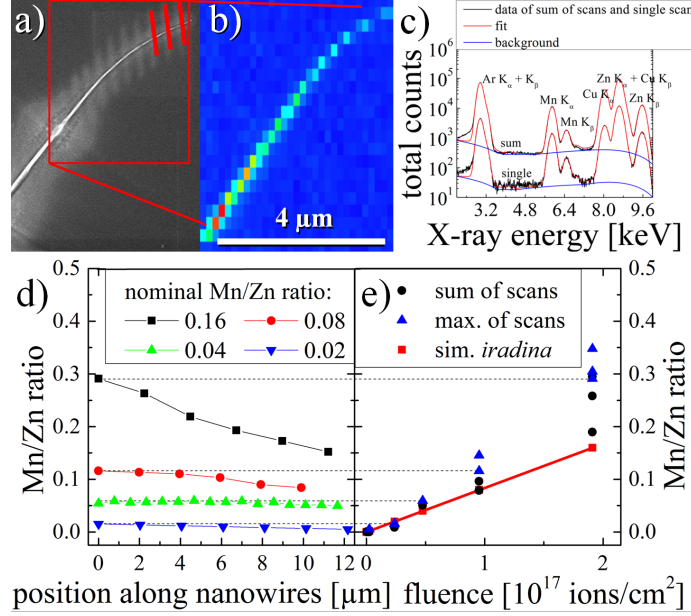


Figure 2.2: a) SEM image of a Mn^+ irradiated ZnO nanowire on the carbon-foil of a Cu TEM grid after XRF investigation. The red lines indicate where the focused X-ray beam was scanned with a long integration time. b) Intensity map of the X-ray signal. c) Exemplary XRF-spectra of a single scanned line and for the sum of all the lines for the nanowire shown in a) and b). d) Mn/Zn ratio quantified with PyMCA for representative wires along the length of the nanowires for varying nominal concentrations. The corresponding data points in the plot of the concentration versus the irradiated ion fluence in e) are connected with a dashed line. The red data points and line in e) indicate the linear extrapolation to the nominal Mn/Zn ratio from *iradina* simulations. The black circles show the average ratio obtained by fitting to the sum of all scans, while the blue upturned triangles show the maximum ratio found for along the length of a nanowire.

2.4 Discussion of relevant effects

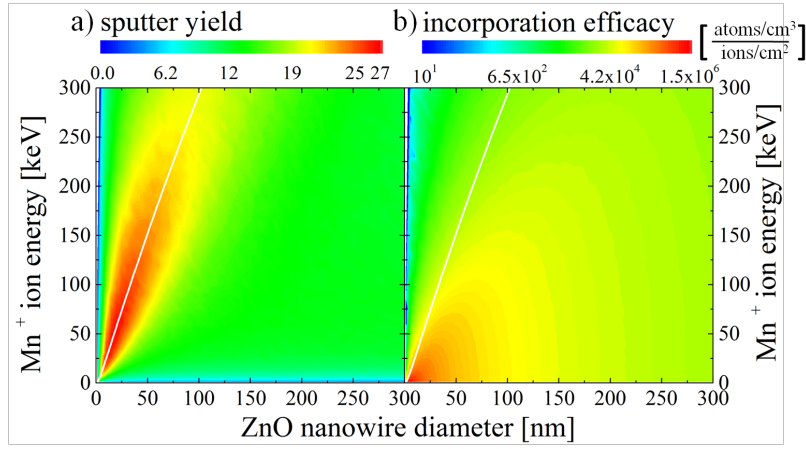


Figure 2.3: a) Sputter yield for the irradiation with Mn^+ of ZnO nanowires with varying diameters and ion energies. From the same simulations the dopant incorporation efficacy was determined and plotted in b). The white line in both plots indicates the ion range at the respective energy and 45° calculated with SRIM for Mn^+ in ZnO .

3 Summary and Outlook

check: Master Thesis Noack, Ogrisek, Conference proceeding D. Sage, Rutherford, Nordlund

Bibliography

- [BMB⁺11] Christian Borschel, Maria E. Messing, Magnus T. Borgstrom, Waldomiro Paschoal, Jesper Wallentin, Sandeep Kumar, Kilian Mergenthaler, Knut Deppert, Carlo M. Canali, Hakan Pettersson, Lars Samuelson, and Carsten Ronning. A New Route toward Semiconductor Nanospintronics: Highly Mn-Doped GaAs Nanowires Realized by Ion-Implantation under Dynamic Annealing Conditions. *Nano Letters*, 11(9):3935–3940, September 2011. WOS:000294790200073.
- [Bor12] Christian Borschel. *Ion-Solid Interaction in Semiconductor Nanowires*. PhD thesis, University Jena, Jena, 2012.
- [JNP⁺14] A. Johannes, S. Noack, W. Paschoal, S. Kumar, D. Jacobsson, H. Pettersson, L. Samuelson, K. A. Dick, G. Martinez-Criado, M. Burghammer, and C. Ronning. Enhanced sputtering and incorporation of Mn in implanted GaAs and ZnO nanowires. *Journal of Physics D-Applied Physics*, 47(39):394003, October 2014. WOS:000341772000005.
- [KPJ⁺13] Sandeep Kumar, Waldomiro Paschoal, Andreas Johannes, Daniel Jacobsson, Christian Borschel, Anna Pertsova, Chih-Han Wang, Maw-Kuen Wu, Carlo M. Canali, Carsten Ronning, Lars Samuelson, and Håkan Pettersson. Magnetic Polarons and Large Negative Magnetoresistance in GaAs Nano-

Bibliography

wires Implanted with Mn Ions. *Nano Letters*, 13(11):5079–5084, 2013.

- [PKB⁺12] Waldomiro Paschoal, Sandeep Kumar, Christian Borschel, Phillip Wu, Carlo M. Canali, Carsten Ronning, Lars Samuelson, and Hakan Pettersson. Hopping Conduction in Mn Ion-Implanted GaAs Nanowires. *Nano Letters*, 12(9):4838–4842, September 2012. WOS:000308576000069.
- [PKJ⁺14] W. Paschoal, Sandeep Kumar, D. Jacobsson, A. Johannes, V. Jain, C. M. Canali, A. Pertsova, C. Ronning, K. A. Dick, L. Samuelson, and H. Pettersson. Magnetoresistance in Mn ion-implanted GaAs:Zn nanowires. *Applied Physics Letters*, 104(15):153112, April 2014. WOS:000335145200060.